Tellus (2003), 55B, 596–612
Printed in UK. All rights reserved

TELLUS
ISSN 0280–6509

A global-scale simulation of the CO_2 exchange between the atmosphere and the terrestrial biosphere with a mechanistic model including stable carbon isotopes, 1953–1999

By AKIHIKO ITO*, *Frontier Research System for Global Change, 3173-25 Showa-machi, Kanazawa-ku, Yokohama 236-0001, Japan*

(Manuscript received 27 December 2001; in final form 27 August 2002)

ABSTRACT

This paper presents the results of a simulation with a mechanistic terrestrial ecosystem model, focusing on the atmosphere–biosphere exchange and stable isotope composition of carbon. The simulation was performed from 1953 to 1999 on the basis of observed climate data and atmospheric carbon dioxide (CO_2) concentration and stable carbon isotope ratio ($\delta^{13}C$). The model, termed Sim-CYCLE, captures carbon dynamics from photosynthetic assimilation to microbial decomposition, including seasonal and interannual variability. Photosynthetic discrimination effect on $\delta^{13}C$ was considered at three levels: (1) leaf-level fractionation, (2) canopy-level CO_2 recycling and (3) continent-level C_3/C_4 pattern. The 47-yr simulation estimated that the average gross CO_2 flux was 121 Pg C yr^{-1}, and that the average photosynthetic $\delta^{13}C$ discrimination coefficient (Δ) was 18.2%. A sensitivity analysis indicated that the estimated Δ depends heavily on the parameterization of stomatal conductance and C_3/C_4 composition. In spite of their small biomass, C_4 plants contributed considerably to the biospheric productivity and belowground carbon supply. The estimated net CO_2 and isotopic exchange of the terrestrial ecosystems corresponded, at least qualitatively, with observed atmospheric CO_2 and its $\delta^{13}C$ seasonal patterns in the Northern Hemisphere. The gross CO_2 fluxes of photosynthesis and respiration indicated a wide range of interannual variability, which was in a sufficient magnitude to induce anomalies in the atmospheric CO_2 growth rate. The estimated Δ showed a wide range of latitudinal and longitudinal variations and seasonal oscillation, but little interannual change. However, during the 47-yr period, the estimated $\delta^{13}C$ of carbon pools decreased by 0.3%, while the $\delta^{13}C$ of atmospheric CO_2 decreased by 0.7%. These results carry implications for the application of a top-down approach, i.e. the double-deconvolution method, to inferring the global terrestrial CO_2 budget.

1. Introduction

The terrestrial biosphere is one of the most important components of the global carbon cycle, and the net CO_2 exchange through photosynthesis and respiration largely affects the spatial and temporal patterns of atmospheric CO_2. However, there remains a large uncertainty in our ability to estimate gross and net CO_2 exchange rates of the terrestrial ecosystems, because of their complexity and heterogeneity (Cramer et al., 1999; Knorr and Heimann, 2001a). It is generally acknowledged that the elucidation of the global carbon cycle, particularly that of terrestrial ecosystems, is a problem of the highest priority (Prentice, 2001), in the face of the global warming induced by human activities (e.g. fossil fuel combustion and land-use change).

The most reliable estimate of the net carbon budget of the terrestrial biosphere was derived from atmospheric data, such as concentration and isotopic composition of CO_2 and O_2/N_2 ratio (Battle et al., 2000). An approach based on the observed atmospheric CO_2

*e-mail: itoh@jamstec.go.jp

concentration and stable carbon isotopic ratio, the so-called double-deconvolution method, was developed to to estimate the net terrestrial and ocean CO_2 budget during the last several decades (Tans et al., 1993; Ciais et al., 1995; Keeling et al., 1995; Francey et al., 1995; Rayner et al., 1999; Morimoto et al., 2000). Hereafter, the stable carbon isotopic composition (^{12}C and ^{13}C) is expressed in parts per thousand ($\delta^{13}C$ in per mill, ‰), defined as follows:

$$\delta^{13}C_{material} = \left(\frac{(^{13}C/^{12}C)_{material}}{(^{13}C/^{12}C)_{standard}} - 1 \right) \times 1000 \qquad (1)$$

where $^{13}C/^{12}C$ is the isotopic ratio, and the standard is carbon dioxide obtained from the PDB. The double-deconvolution method is based on there being significant difference in the magnitude of the $\delta^{13}C$ discrimination effect between the terrestrial–atmosphere and ocean–atmosphere CO_2 exchange processes. Because this is a top-down approach, we can obtain a set of simultaneous equations with respect to the net CO_2 exchange rate between the land biosphere and the ocean. It is important that we should, at least ideally, know the spatio–temporal distribution of both the concentration and stable carbon isotope ratio of the atmospheric CO_2 at an equivalent level of precision. However, compared with the concentration, we have much less information on the stable carbon isotope composition, because of practical difficulties in quantification with mass spectrometers. We are aware that the relative weakness of $\delta^{13}C$ precision may be partly responsible for the discrepancies among the double-deconvolution studies (e.g. Keeling et al., 1995; Francey et al., 1995). Moreover, there are a relatively small number of modeling studies on the isotopic features of the atmosphere–biosphere CO_2 exchange (Lloyd and Farquhar, 1994; Ciais et al., 1995; Fung et al., 1997; Wittenberg and Esser, 1997; Ciais et al., 1999; François et al., 1999). For example, Fung et al. (1997) adopted the Simple Biosphere-2 and Carnegie–Ames–Stanford Approach (SiB2/CASA), coupled with an atmosphere model, to evaluate the effect of terrestrial ecosystems on the $\delta^{13}C$ of atmospheric CO_2. However, among the more than 20 models developed to date (Cramer et al., 1999), only a few models apply to the estimation of both carbon exchange and isotopic dynamics of the terrestrial biosphere (e.g. SiB2/CASA by Fung et al., 1997; BIOME-3.5 by Buchmann and Kaplan, 2001; Lund–Potsdam–Jena model by Sitch, 2000). Thus, developing models and performing simulations of terrestrial effects on the $\delta^{13}C$ of atmospheric CO_2 is a challenge for us.

In this study, the atmosphere–biosphere exchange and stable carbon isotopic ratio of CO_2 were simulated on a global scale by using a mechanistic model. The inclusion of the isotopic ratio into the model is expected to supply additional aspects of the functioning of terrestrial ecosystems, and then is effective for the validation of the model with other supporting evidence. We could include processes related to $\delta^{13}C$ into the terrestrial ecosystem model, referring to physiological, ecological and biogeochemical studies. Spatial distribution, seasonal change, and interannual changes are addressed on the basis of a biome map and climate time-series data for a recent 47-yr period. The response of the terrestrial carbon budget to the past rapid CO_2 increase and $\delta^{13}C$ decrease is also discussed in terms of disequilibrium between the atmosphere and biosphere.

2. Methods

2.1. Carbon dynamics in terrestrial ecosystems

A process-based model, Sim-CYCLE (Simulation model of Carbon cYCle in Land Ecosystems), was used to capture the carbon dynamics of terrestrial ecosystems. In the model (Fig. 1), carbon storage is divided into five compartments: W_F, leaves; W_C, stems; W_R, roots; W_L, litter, or dead phytomass; and W_H, humus, or soil organic matter. Atmospheric CO_2 is conveniently divided into that in the free atmosphere and that within the canopy boundary layer. Sixteen carbon flows among the carbon pools represent ecosystem processes, including photosynthetic production, reproduction, respiratory metabolism, mortality and decomposition. Importantly, plant carbon pools and fluxes are divided into C_3- and C_4-plant components, because of discrepancies in environmental responsiveness and stable carbon isotopic composition between the two plant groups [here, crassulacean acid metabolism (CAM) plants were not explicitly considered]. The ecosystem processes (production, growth and succession) are parameterized in a mechanistic manner, on the basis of dry-matter production theory and physiological regulations (Ito and Oikawa, 2002). Sim-CYCLE includes a water and energy budget submodule, in which net radiation, evaporation, runoff and soil moisture content are estimated with an arbitrary time-step. The model has actually been used to analyze the relationship between climatic perturbations

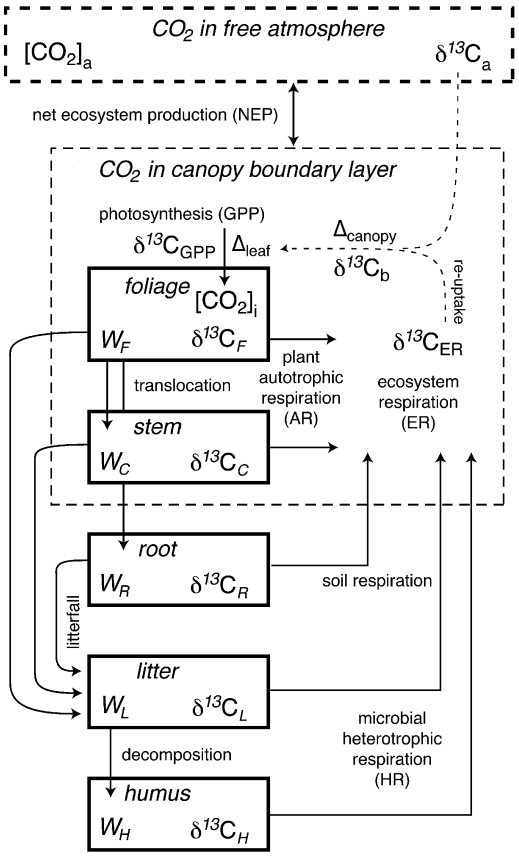

Fig. 1. Schematic diagram of the atmosphere–biosphere CO_2 exchange and intraecosystem carbon dynamics, as adopted in a process-based model, Sim-CYCLE. Note that plant compartments (foliage, stem, and root) were internally separated into C_3- and C_4-plant components for herbaceous biomes (see Table 1). All carbon fluxes and pools are characterized by the stable carbon isotope ratio ($\delta^{13}C$), simultaneously calculated with the carbon dynamics simulation.

and the net ecosystem CO_2 budget (Ito and Oikawa, 2000a, b).

Gross photosynthetic production (GPP) is primarily a function of available photosynthetically active radiation, and is modulated by several environmental factors, such as leaf temperature, ambient air humidity, soil moisture availability and atmospheric CO_2 concentration. These environmental dependencies were basically formulated at the leaf level, and then scaled up to the level of canopy, taking light attenuation within the canopy into account. Ecosystem respiration (ER) is composed of plant and soil components, i.e. autotrophic respiration (AR) and heterotrophic respiration (HR). AR is a function of surface temperature and biomass growth rate, and HR is a function of soil temperature and soil moisture content. For example, AR and HR are expected to increase exponentially with increasing temperature. The specific respiration capacity under the standard environmental condition is different among the carbon compartments and biomes. To characterize biomes and C_3/C_4 plants, different ecophysiological parameters were given.

Net exchange of CO_2 between the atmosphere and terrestrial ecosystems is termed net ecosystem production (NEP):

$$\mathrm{NEP} = \mathrm{GPP} - \mathrm{AR} - \mathrm{HR} \tag{2}$$

Clearly, NEP is a compound function of temperature, moisture, radiation and atmospheric CO_2 concentration. Net primary production (NPP), frequently used in ecological and carbon cycle research, is readily derived as the difference between GPP and AR. It is noted that the present simulation does not consider carbon flows caused by disturbances and human activities, such as wildfire and exploitation. Other ecosystem processes, such as senescence, allocation and phenology, are also included in Sim-CYCLE, and are fully described by Ito and Oikawa (2002). Because Sim-CYCLE is a simple one-dimensional model, one can easily perform a long-term integration for decades and centuries.

2.2. Stable carbon isotopes

2.2.1. Inclusion of the stable carbon isotopic ratio. The $\delta^{13}C$ values of the various biospheric carbon pools were denoted with subscripts, e.g. $\delta^{13}C_F$ for foliage and $\delta^{13}C_{AR}$ for CO_2 respired from plant biomass (see Fig. 1). Therefore, along with the net ecosystem CO_2 exchange, isotopic flux (isoflux) is conveniently defined as a $\delta^{13}C$-weighted NEP ($\mathrm{NEP}_{\mathrm{isoflux}}$):

$$\begin{aligned}\mathrm{NEP}_{\mathrm{isoflux}} &= \delta^{13}C_{GPP}\cdot\mathrm{GPP} - \delta^{13}C_{AR}\cdot\mathrm{AR} \\ &\quad - \delta^{13}C_{HR}\cdot\mathrm{HR} \\ &= \delta^{13}C_{GPP}\cdot\mathrm{GPP} - \delta^{13}C_{ER}\cdot\mathrm{ER}.\end{aligned} \tag{3}$$

While a negative NEP means a net CO_2 emission from the biosphere, a negative $\mathrm{NEP}_{\mathrm{isoflux}}$ means a net discrimination against ^{13}C.

As an approximation, it was assumed that significant $\delta^{13}C$ fractionation takes place in photosynthetic CO_2 assimilation, and that fractionation in biosynthesis, respiration and decomposition is sufficiently

small to be neglected by the simulation study (Lin and Ehleringer, 1997; Ågren et al., 1996). Therefore, $\delta^{13}C$ values of respired CO_2 (e.g. $\delta^{13}C_{AR}$ and $\delta^{13}C_{HR}$) are identical to those of the source carbon pools, whose $\delta^{13}C$ values are updated at every time-step. Here, isotopic composition of assimilated carbon ($\delta^{13}C_{GPP}$) is calculated as follows:

$$\begin{aligned}\delta^{13}C_{GPP} &= \delta^{13}C_a - \Delta \\ &= \left(\delta^{13}C_a - \Delta_{canopy}\right) - \Delta_{leaf} \\ &= \delta^{13}C_b - \Delta_{leaf}\end{aligned} \quad (4)$$

where Δ, Δ_{canopy} and Δ_{leaf} denote the total canopy-level, and leaf-level photosynthetic $\delta^{13}C$ discrimination coefficients, respectively. [Note that the definition of Δ is slightly different from that of Farquhar et al. (1989), but this may not lead to a significant difference]. Globally, $\delta^{13}C_{GPP}$ depends on three factors: (1) leaf-level fractionation due to different diffusion velocities and enzymatic affinity, (2) the degree of re-uptake of respired CO_2 within the canopy, leading to condensation of the lighter isotope and (3) geographic distribution of C_3 and C_4 plants. Each factor was parameterized as described below, and their relative importance is addressed by a sensitivity study. Here, sensitivity of Δ was examined in response to $\pm 10\%$ change in these parameters: stomatal conductance, canopy recycling and C_4 plant coverage, related to ^{13}C discrimination, and plant mortality and soil decomposition rate, related to carbon turnover in terrestrial ecosystems.

2.2.2. Leaf-level discrimination. Through many ecophysiological studies (e.g., O'Leary et al., 1986; Farquhar et al., 1989), the relationships and mechanisms of leaf-level gas exchange and isotopic fractionation have been almost elucidated. In particular, we should note that there are apparent differences in Δ_{leaf} between C_3 and C_4 plants. These studies suggest that $\delta^{13}C$ fractionation factor of C_3 and C_4 species (Δ_{leaf}) can be respectively given as functions of the ratio of CO_2 concentrations between ambient air ($[CO_2]_a$) and intercellular space of the plant leaves ($[CO_2]_i$):

$$C_3: \ \Delta_{leaf} = a + (b - a)\frac{[CO_2]_i}{[CO_2]_a} \quad (5)$$

$$C_4: \ \Delta_{leaf} = a + (c + \phi b - a)\frac{[CO_2]_i}{[CO_2]_a} \quad (6)$$

where a denotes discrimination fraction related to diffusion (4.4%), b denotes discrimination related to carboxylation by ribulose bisphosphate carboxylase-oxygenase (RuBisCO) (27% for C_3 and 30% for C_4), c represents discrimination related to carboxylation by phosphoenol pyruvate (PEP) carboxylase (−5.7%), and ϕ is the leakage fraction from bundle sheath cells (0.21). Equations (5) and (6) are applied to all C_3 and C_4 plants, irrespective of biome types. The basic relationship among photosynthetic rate, stomatal conductance, and intercellular CO_2 concentration was:

$$[CO_2]_i = [CO_2]_a - \frac{P}{g_s} \quad (7)$$

where P denotes the single-leaf photosynthetic rate, which is characterized by the light-saturated photosynthetic rate, light-use efficiency and photosynthetically active radiation (for details, see Ito and Oikawa, 2002). Stomatal conductance (g_s), one of the critical parameters characterizing ecosystem function, was based on a semi-empirical model by Leuning (1990). For scaling-up, Sim-CYCLE regards canopy as a single big-leaf, by integrating for leaf area index of the canopy (Ito and Oikawa, 2002). In practice, P, g_s and $[CO_2]_i$ were deduced by an iterative calculation to obtain an equilibrium leaf-level gas exchange.

2.2.3. Canopy-level: CO_2-recycling. If a part of the respired CO_2 from plants and soils is assimilated within the canopy before escaping into the free atmosphere, the isotopic fractionation effect becomes larger than would be expected solely at the leaf-level (Keeling, 1961). For example, Sternberg et al. (1997) suggest that up to 39% of respired CO_2 can be assimilated again in a dense tropical rain forest at a low wind velocity. Thus, we should introduce a canopy-level $\delta^{13}C$-discrimination coefficient (Δ_{canopy}):

$$\Delta_{canopy} = \delta^{13}C_a - \delta^{13}C_b \quad (8)$$

where $\delta^{13}C_a$ and $\delta^{13}C_b$ represent $\delta^{13}C$ values of CO_2 in the free atmosphere and canopy boundary layer, respectively (cf. Fig. 1). Several model studies have addressed CO_2 recycling in the canopy (Lloyd et al., 1996; Buchmann and Kaplan, 2001). Here, a simple mixing-ratio model was used:

$$\delta^{13}C_b = (1 - \sigma)\,\delta^{13}C_a + \sigma\,\delta^{13}C_{ER}. \quad (9)$$

It follows that the magnitude of CO_2 recycling (σ) would increase as (1) the canopy becomes dense and is decoupled from the atmosphere; (2) wind velocity becomes low, reducing turbulent transportation; and (3) plants and soils supplies CO_2 actively, diluting atmospheric CO_2 with respired CO_2. In this study, Δ_{canopy} was assumed to increase as the leaf area index, LAI, and the ecosystem respiration rate, ER, increased. For

Table 1. *Biome classification and area distribution adopted for simulation (after Matthews, 1983)*

Biome	Area (10^6 km^2)			Photosynthetic pathway
	Potential	Actual	Cultivated (pot. – act.)	
Tropical evergreen rainforest	16.5	15.5	1.0	C_3
Ssubtropical evergreen rainforest	0.2	0.2	0.0	C_3
Tropical/subtropical drought-deciduous forest	3.8	2.8	1.0	C_3
Temperate evergreen seasonal broadleaved forest, summer rain	1.2	0.8	0.4	C_3
Evergreen broadleaved sclerophyllous forest, winter rain	0.5	0.3	0.1	C_3
Tropical/subtropical evergreen needle-leaved forest	0.7	0.6	0.1	C_3
Temperate/subpolar evergreen rainforest	0.3	0.2	0.0	C_3
Temperate/subpolar evergreen needle-leaved forest	10.3	9.9	0.5	C_3
Cold-deciduous forest, with evergreens	15.4	11.3	4.2	C_3
Xeromorphic forest/woodland	5.2	4.9	0.4	C_3
Tropical/subtropical drought-deciduous woodland	5.1	4.1	1.0	C_3/C_4
Evergreen broadleaved shrubland, evergreen dwarf-shrubland	12.5	11.7	0.8	C_3/C_4
Ddrought-deciduous shrubland	0.9	0.8	0.1	C_3
Cold-deciduous woodland	3.1	3.0	0.1	C_3
Tall/medium/short grassland, 10–40% woody cover	18.6	15.4	3.2	C_3/C_4
Tall/medium/short grassland, <10% woody cover	13.5	10.6	2.9	C_3/C_4
Arctic/alpine tundra, mossy bog	6.5	6.5	0.0	C_3
Desert	14.9	14.6	0.3	C_3/C_4
Ice	14.5	14.5	0.0	–
Total	143.6	127.6	16.0	

example, in a typical tropical rain forest (LAI = 6), about 16% of ecosystem respiration was fixed again, leading to the Δ_{canopy} value of 2.7%. Because the time-step of the simulation (i.e. monthly) was too long to capture the wind effect accurately, the upper limit of CO_2 recycling was arbitrarily limited to <20%.

2.2.4. Continent-level discrimination: geography of C_3 and C_4 plants. The composition of C_3 and C_4 plants was considered to be their fractional area occupancies, by which the mixed C_3/C_4 flux was weighted. It could be assumed that forest ecosystems were initially composed exclusively of C_3 plants, and that C_4-plant distribution was limited to savanna, grassland and desert biomes (see Table 1).

Many observations suggest that temperature is the most influential environmental factor affecting the geographical distribution of C_3 and C_4 plants in grassland biomes, and that moisture availability exerts an ancillary effect (Paruelo and Lauenroth, 1996; Sage et al., 1999). Teeri and Stowe (1976) suggested that C_4-plant dominance in the North America may increase linearly, as temperature (e.g. the mean growing-period temperature) becomes warmer. A similar relationship has been observed in many regions: central Asia (Winter, 1981), South America (Cavagnaro, 1988), Australia (Hattersley, 1983), middle Afirica (Tieszen et al., 1979), and East Asia (Takeda et al., 1985). Ehleringer et al. (1997) attributed the physiological mechanism of this robust relationship to the temperature dependence of photosynthetic quantum yield, or light-use efficiency. In addition to the geographic gradient, several observations in temperate regions revealed that there is a seasonal variation in the C_3 and C_4 composition, such that C_4 plants are liable to dominate the community in the dry summer season (Caldwell et al., 1977; Saigusa et al., 1996).

At present, there is no general mechanistic model for estimating grassland C_3/C_4 composition, and then an empirical model based on the above observations was employed in this study. At first, the seasonal maximum C_4 dominance $fC_{4,max}$ (fraction) was assumed as a linear function of annual mean temperature (T_{ann}), as follows:

$$fC_{4,max} = 0.15 + 0.04T_{ann}. \quad (10)$$

In consequence, C_4 plants were almost precluded from higher latitudes (>55°N), and C_3–C_4 crossover (equivalent dominance) occurred around 30°N and S with longitudinal and seasonal variations. Then, monthly

value (fC_4) was obtained by modulating with coefficients of monthly temperature (T_{mon}) and monthly precipitation (P_{mon}):

$$fC_4 = fC_{4,max} f_T(T_{mon}) f_P(P_{mon}) \quad (11)$$

$$f_T(T_{mon}) = 1/\{1 + \exp[-0.22(T_{mon} - 12.5)]\} \quad (12)$$

$$f_P(P_{mon}) = 1/\{1 + \exp[0.0105(P_{mon} - 400)]\}. \quad (13)$$

The coefficients $f_T(T_{mon})$ and $f_P(P_{mon})$ bring about a seasonal change, such that warmer and drier conditions favor C_4 plants. In tropical grasslands, C_4 plants predominate all the year round.

2.3. Input data

Forcing environmental variables were given as a prescribed scenario (i.e. no feedback from the simulation result), derived from observations. Climatic conditions from 1953 to 1999 were derived from a reanalysis dataset of the US National Centers for Environmental Prediction (NCEP) and the National Center for Atmospheric Research (NCAR). The dataset gives monthly average values for surface meteorology, such as downward short-wave radiation, cloud cover, air specific humidity, precipitation, air temperature, surface temperature, soil temperature (at 0–10 and 10–200 cm depth) and wind velocity. Atmospheric CO_2 concentration ($[CO_2]_a$) and stable carbon isotope ratio ($\delta^{13}C_a$) was derived from observations by Keeling and Whorf (2000) and GLOBALVIEW–CO_2 (2000). In this case, $[CO_2]_a$ increased from 313 ppmv in 1953 to 369 ppmv in 1999, and $\delta^{13}C_a$ decreased from -7.0% to -7.8%, with a seasonal oscillation and latitudinal gradient. During the spin-up period, a pre-industrial $[CO_2]_a$ (280 ppmv) and $\delta^{13}C_a$ (–6.5%) were assumed, based on ice-core analyses by Friedli et al. (1986), Etheridge et al. (1996), and Francey et al. (1999).

Global maps of natural vegetation and cultivation intensity (Matthews, 1983) were used to determine the actual biome distribution. For the present purpose, the biome classification was simplified into 19 types (Table 1). Since the numerical experiment was carried out at the spatial resolution of the NCEP/NCAR-reanalysis dataset, i.e. a T62 Gaussian grid (94 latitudinal zones and 192 longitudinal columns), the biome dataset was adjusted to that resolution by re-sampling of grid points. Calculations were carried out for natural vegetation and cropland independently, and their area-weighted average represents the carbon dynamics at each grid point (Ito and Oikawa, 2000b).

2.4. Calibration, validation and simulation design

Through two lines of comparison procedures, the model parameters were calibrated (Ito and Oikawa, 2002): an extensive one at global 21 sites, and an intensive one at four sites. In the extensive comparison, the model results of net primary production, plant biomass, leaf area index and soil carbon storage were compared with observations. It was found that the model indicates good agreements with observations, confirming model applicability to a wide variety of terrestrial ecosystems from tropical rain forest to tundra. In the intensive comparison, all carbon flows and pools were individually compared with observations at four sites (one each in a tropical, temperate, boreal forest and grassland biome). This confirmed the model reliability that Sim-CYCLE is a robust tool to retrieve the atmosphere–biosphere carbon exchange and intra-system carbon dynamics. In this study, a top-down examination of model performance was also carried out, to examine how biospheric exchange affects atmospheric CO_2. The estimated zonal mean NEP and $NEP_{isoflux}$ values (accumulated seasonally) were compared with observed CO_2 and $\delta^{13}C_a$, at Point Barrow (lat 71°19′N) and Niwot Ridge (lat 40°03′N) (GLOBALVIEW–CO_2, 2000). This test allowed us to examine correspondence between seasonal phases and to compare two distant sites, in a qualitative manner.

The numerical experiment during the period from 1953 to 1999 was carried out, after a sufficient length of spin-up and transitional period. The spin-up integration as long as 4000 yr was performed, in order to obtain an equilibrium state of terrestrial carbon dynamics under a stationary condition (pre-industrial CO_2 but no difference in climate). Then, taking about 50 yr, atmospheric CO_2 condition was transitionally adjusted to the level at the beginning of the experiment, i.e. in 1953, to avoid an artifact caused by an abrupt conditional shift from spin-up to experiment.

3. Results and discussion

3.1. Overview of the carbon budget

Throughout the experimental period (1953–1999), average gross CO_2 fluxes between the atmosphere and

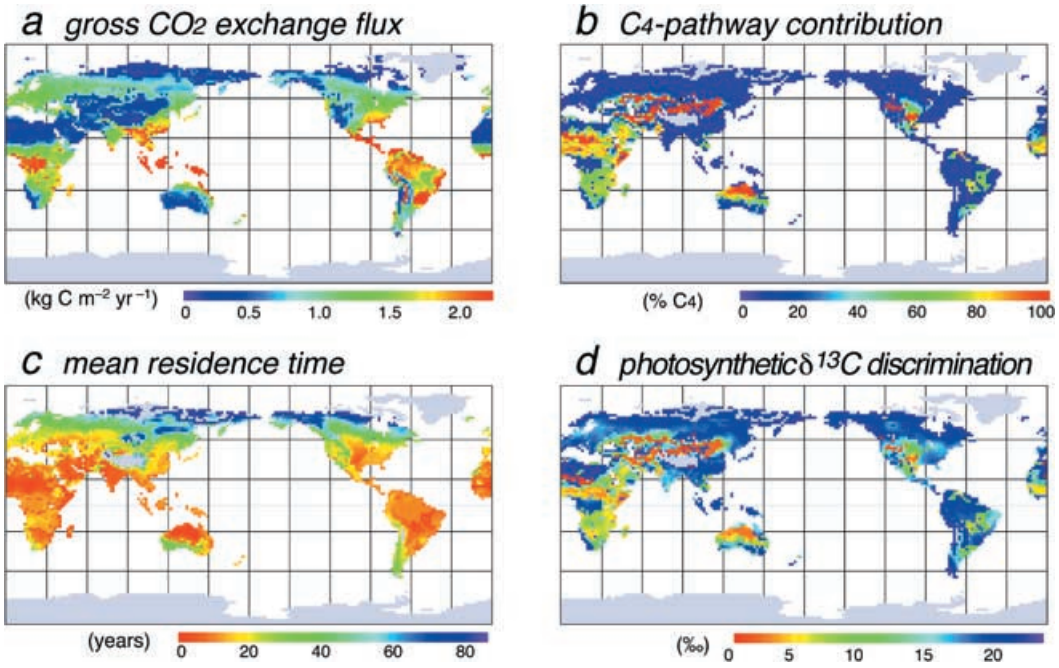

Fig. 2. Distribution of estimated atmosphere–biosphere CO_2 exchange properties, averaged for the period from 1953 to 1999. Annual (a) gross CO_2 exchange rate through photosynthetic uptake (GPP) or respiratory release (ER), (b) contribution of C_4 pathway to the gross fluxes, (c) mean residence time of the CO_2-derived carbon in terrestrial ecosystems, and (d) $\delta_{13}C$ fractionation effect, weighted by C_3 and C_4 photosynthetic rates.

the terrestrial biosphere, GPP, AR and HR, were estimated as 121.5, 59.4 and 60.5 Pg C yr^{-1} (Pg = 10^{15} g). Therefore, the average global NPP was 62.1 Pg C yr^{-1}. The gross CO_2 flux occurred heterogeneously over the biosphere, with values ranging from those in the tropical rain forest (>2.0 kg C m^{-2} yr^{-1}) to tundra and desert values (<0.1 kg C m^{-2} yr^{-1}) (Fig. 2a). The contribution ratio by C_4 plants to the global annual GPP was estimated as 21.1 ± 0.5% (standard deviation, interannual variability); this is consistent with other estimates, e.g. 20.8% by Lloyd and Farquhar (1994) and 17.0% by Wittenberg and Esser (1997). As shown in Fig. 2b, the C_4 contribution was higher (>80%) in hot arid grasslands, such as Australia, eastern Afirica, Central Asia and central North America. This result is consistent with observations that C_4 plants have higher contribution to ecosystem productivity in lower grasslands (Epstein et al., 1997).

Total carbon stocks in W_F, W_C, W_R, W_L and W_H were estimated as 40.7, 675.0, 132.5, 59.1 and 1448.4 Pg C, respectively. The stem and root biomass was dominated by woody forest species, while C_4 plants accounted for only 2.3% of the global biomass storage, in spite of their wide area occupancy (Table 2). However, 20.3% of total leaf mass was attributable to C_4 plants, and 8.7% of soil organic matter to C_4-derived carbohydrates. Accordingly, C_4 plants may play a quantitatively important role in the global carbon cycle. On the basis of gross flux and carbon accumulation, we could infer a mean residence time (MRT) of biospheric carbon storage. However, the single average MRT value, 19.7 yr (= total storage/gross flux), is misleading, because MRT varies widely among terrestrial ecosystems, from 5 to more than 100 yr (Fig. 2c). Remarkably, in most ecosystems, the MRT for foliage and litter was estimated as less than 2 yr, allowing them to reflect changes in atmospheric CO_2 parameters without delay. Because humus had the longest MRT, the estimated $\delta^{13}C_H$ values were higher (less negative) than $\delta^{13}C_L$ by 0.48‰ on an average, leading to a vertical gradient in $\delta^{13}C$ in the profile of soil organic carbon, as has been captured by field surveys (Ehleringer et al., 2000).

The average stable carbon isotopic ratio of ecosystem respiration ($\delta^{13}C_{ER}$) was estimated as −25.5‰; this model estimation is in good agreement with

Table 2. *Summary of the simulation of atmosphere-biosphere CO_2 exchange with a stable-C-isotope-coupled Sim-CYCLE, for the first and the last 10 yr of the numerical experiment*

	Unit	1953–62	1990–99
Area coverage of vegetation	10^6 km^2	129.1	129.1
(C_4 plants)	%	29.5	29.6
Plant biomass C, total	Pg C	836	864
(C_4-derived)	%	2.3	2.3
Soil organic C, total	Pg C	1492	1519
(C_4-derived)	%	8.8	8.6
Gross photosynthetic production, GPP	Pg C yr^{-1}	119.8	124.3
(C_4-derived)	%	20.6	21.1
Autotrophic respiration, AR	Pg C yr^{-1}	58.6	60.7
Net primary production, NPP	Pg C yr^{-1}	61.2	63.6
Heterotrophic respiration, HR	Pg C yr^{-1}	59.6	61.5
Net ecosystem production, NEP	Pg C yr^{-1}	1.6	2.1
δ^{13}C of the biospheric C	‰	−27.8	−28.1
δ^{13}C of C_3 plant C	‰	−29.3	−29.8
δ^{13}C of C_4 plant C	‰	−10.5	−11.2
δ^{13}C of soil C	‰	−27.6	−27.8

observational one by Buchman and Kaplan (2001), −25.3‰. Thus, respired CO_2 was isotopically heavier than the average biospheric carbon storage (about –28‰, Table 2), because C_3-derived lighter carbon predominates the biospheric carbon pools with longer MRTs, such as woody stems and soil humus in higher latitudes. The isotopic difference between carbon storage and respired CO_2 may lead to some estimation error, if a double-deconvolution study neglect the difference (Tans et al., 1993).

3.2. *Discrimination effect (Δ) and sensitivity analysis*

The biospheric average of photosynthetic δ^{13}C discrimination (Δ), 18.2 ± 0.1‰, seems sufficiently close to that commonly used in carbon cycle studies (18.0‰; Keeling et al., 1989), but it is slightly larger than that derived from a recent atmospheric observations (16.8‰; Bakwin et al., 1998). This Δ value is equivalent to a $^{13}C/(^{13}C + {}^{12}C)$ discrimination coefficient of 0.98184, and a $^{13}C/^{12}C$ discrimination coefficient of 0.98164. C_3 and C_4 plants exerted disparate effects on photosynthetic δ^{13}C discrimination: on average 19.8‰ for C_3 and 2.5‰ for C_4 plants (Fig. 3). The Δ value of C_3 plants ranges from 12.0‰ to 26.5‰ in accordance with the wide distribution and diversity of C_3 plants (Fig. 2d). From eqs. (5) and (6), the average $[CO_2]_i/[CO_2]_a$ ratio was calculated as 0.68 for C_3 plants and 0.51 for C_4 plants. The lower $[CO_2]_i$ of C_4 plants is attributable to their higher photosynthetic rate (P) and lower stomatal conductance (g_s) than those of C_3 plants [cf. eq. (7)]. Also, as can be seen in Fig. 3, CO_2 recycling within the canopy resulted in larger δ^{13}C discrimination (average 2.1‰). The canopy-level effect (Δ_{canopy}) was especially large

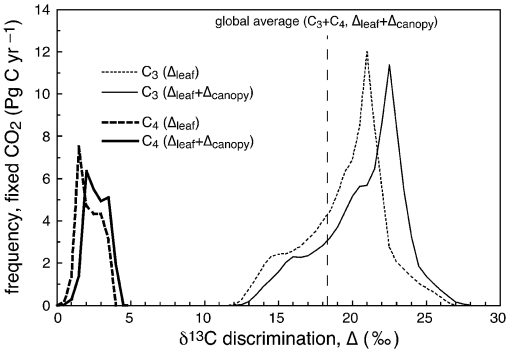

Fig. 3. Frequency distribution of photosynthetic δ^{13}C fractionation of the global land vegetation with C_3 or C_4 pathways, as captured by the Sim-CYCLE simulation for the period from 1953 to 1999. Note that the discrimination effect depends here on both leaf-level gas diffusion and CO_2 recycling in the plant canopy.

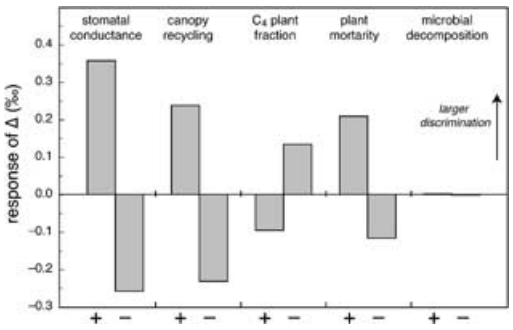

Fig. 4. Sensitivity of the annual biospheric Δ, in response to ±10% uncertainties in processes relevant to photosynthetic δ^{13}C discrimination and carbon turnover.

in tropical forests with thick canopies and active respiratory efflux from plants and soil.

The sensitivity analysis implied that Δ is so sensitive to the discrimination processes that their uncertainty could lead to significant estimation errors (Fig. 4). Increased stomatal conductance and canopy recycling resulted in higher Δ values, whereas increased C_4 coverage lead to smaller discrimination effect. It seems that stomatal conductance (g_s) exerted the largest effect on the estimated Δ; i.e. 10% uncertainty in stomatal conductance resulted in up to 0.3‰ change in Δ, because g_s can strongly affect the $[CO_2]_i/[CO_2]_a$ ratio [cf. eq. (7)]. Therefore, determining stomatal conductance should be important not only for quantifying the CO_2 assimilation rate, but also for constraining the photosynthetic δ^{13}C discrimination effect, ranging from single-leaf to the global scale. The canopy recycling and C_3/C_4 plant composition could exert moderate influences on Δ (0.1 to 0.2‰ in response to 10% variation). In addition, plant mortality could moderately affect the estimated Δ, while soil decomposition rate had little effect. The sensitivity to plant mortality is due to altered C_3/C_4 contribution, rather than single-leaf and canopy processes. In this case, the impacts of increased mortality, leading to smaller LAI and GPP, were more evident in sparse grasslands than in dense forests. As a result, contribution ratio of C_4 plants declined, enlarging the discrimination coefficient. In sum, the sensitivity analysis was effective for identifying critical processes and parameters, and implicative to internal uncertainties within the model. Further analyses with respect to other carbon dynamics and ecophysiological parameters will be done elsewhere.

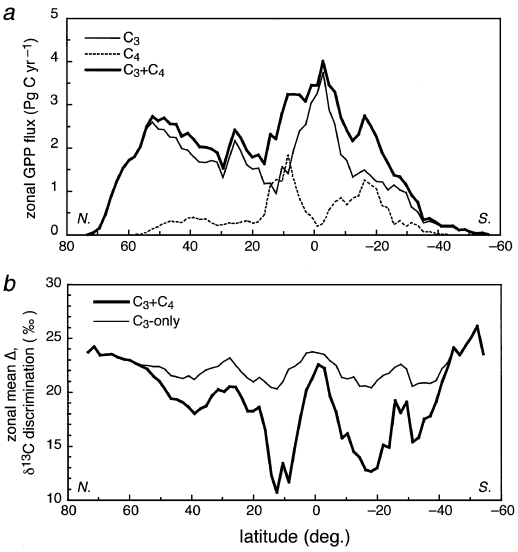

Fig. 5. Estimated latitudinal variations in (a) the gross photosynthetic CO_2 uptake rates by C_3 and C_4 plants and (b) the photosynthetic δ^{13}C-discrimination coefficient (Δ) of terrestrial ecosystems compared with atmospheric CO_2. Averaged over the experimental period from 1953 to 1999, for 94 latitudinal zones.

3.3. *Latitudinal variation*

A latitudinal aggregation of the biospheric CO_2 and δ^{13}C exchange clearly exemplifies the heterogeneity of the terrestrial biosphere. The photosynthetic δ^{13}C discrimination coefficient varied latitudinally, such that Δ was smaller near the subtropical latitudes (around 18°N and S) (Fig. 5), where C_4 plants predominate in savanna and subtropical grasslands (Fig. 2b). Near the equator, tropical rain forest dominated the zonal GPP, and therefore zonal Δ came close to the values for C_3 plants. The latitudinal variation in the relative abundance of C_3 and C_4 plants may be partly responsible for the latitudinal change in the $[CO_2]_a - \delta^{13}C_a$ relationship, along with the effect of the oceanic exchange, as observed by Nakazawa et al. (1997).

Ecological surveys have also addressed the latitudinal gradients in terms of the biospheric δ^{13}C characteristics. For example, in the Great Plains (North America), Epstein et al. (1997) showed with a regression model a similar latitudinal change in the relative dominance of C_3 and C_4 plants in terms of productivity. Tieszen et al. (1997) suggest that soil organic matter also shows a δ^{13}C gradient, from −14‰ at lat. 30°N to −25‰ at lat. 50°N, because of the C_3/C_4

composition change. On the other hand, Körner et al. (1991) showed that there is a latitudinal gradient in the leaf-level discrimination factor, such that the Δ_{leaf} value of C_3 plants becomes smaller with ascending latitude and altitude. Bird et al. (1996) suggested that the $\delta^{13}C$ value of soil organic matter shows a latitudinal gradient related to differences in mean residence time. That is, soil organic matters at high latitudes is liable to take higher (less negative) $\delta^{13}C$ values, because of slower decomposition and longer MRTs, allowing old carbon to persist in the soil (Fig. 2c). Such ecological evidence will serve to validate the model estimates.

3.4. Seasonal change

Total GPP changed seasonally from 6.6 Pg C month^{-1} in February to 15.5 Pg C month^{-1} in July, apparently driven by the seasonal change in the Northern Hemisphere (Fig. 6). The Northern Hemisphere was characterized by the apparent seasonal variation in the relative C_3 and C_4 contributions, while the Southern Hemisphere had only a little seasonal change in the C_3/C_4 contribution ratio. In the Northern Hemisphere, GPP of both C_3 and C_4 plants became large in summer, but the amplitude of C_3 plants was quantitatively larger than that of C_4 plants (Fig. 6a). In consequence, the contribution ratio of C_4 plants decreased in summer, leading to larger biospheric discrimination. The marked increase in the C_3-derived GPP was attributable to the vast area with temperate forest, boreal forest and spring-cultivated cropland. Ecosystem respiration (ER) also changed seasonally, in phase with the change in GPP (Fig. 6b). The contribution by C_4 plants to monthly plant respiration (AR) became larger in the northern winter, leading to an isotopically heavier CO_2 efflux into the atmosphere. The seasonal change in the relative C_3/C_4 contribution led to a seasonal oscillation in the photosynthetic fractionation coefficient Δ, even at the global scale, from 17.0‰ in February to 18.8‰ in August (Fig. 7). When examined in relation to latitudinal zone, seasonal variability in Δ reached as high as 5‰.

As clearly shown by previous observations (Keeling et al., 1989; Nakazawa et al., 1997), atmospheric CO_2 concentration ($[CO_2]_a$) and its stable carbon isotope ratio ($\delta^{13}C_a$) show similar seasonal changes, but in the opposite phase. Also, the amplitude of the seasonal changes becomes larger at higher

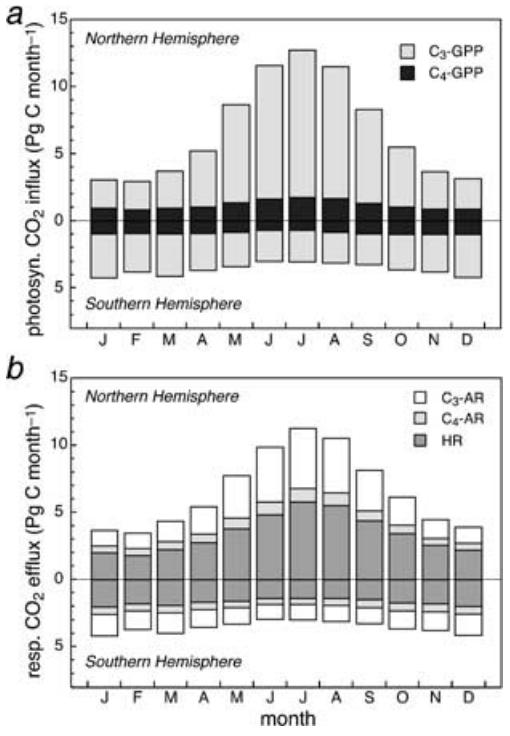

Fig. 6. Estimated seasonal changes in (a) photosynthetic CO_2 uptake by C_3 and C_4 plants, and (b) respiratory CO_2 release from C_3/C_4 plants and soil. Contributions by the Northern and Southern Hemisphere are cumulatively divided in each column.

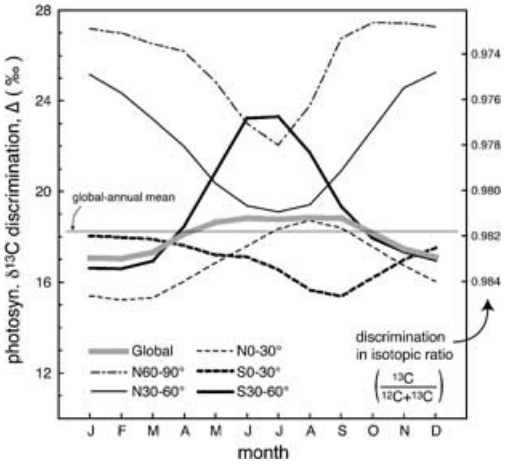

Fig. 7. Estimated seasonal changes in the photosynthetic $\delta^{13}C$ discrimination effect of terrestrial ecosystems (including both C_3 and C_4 plants), averaged for the period from 1953 to 1999. Zonal and global averaged values are shown.

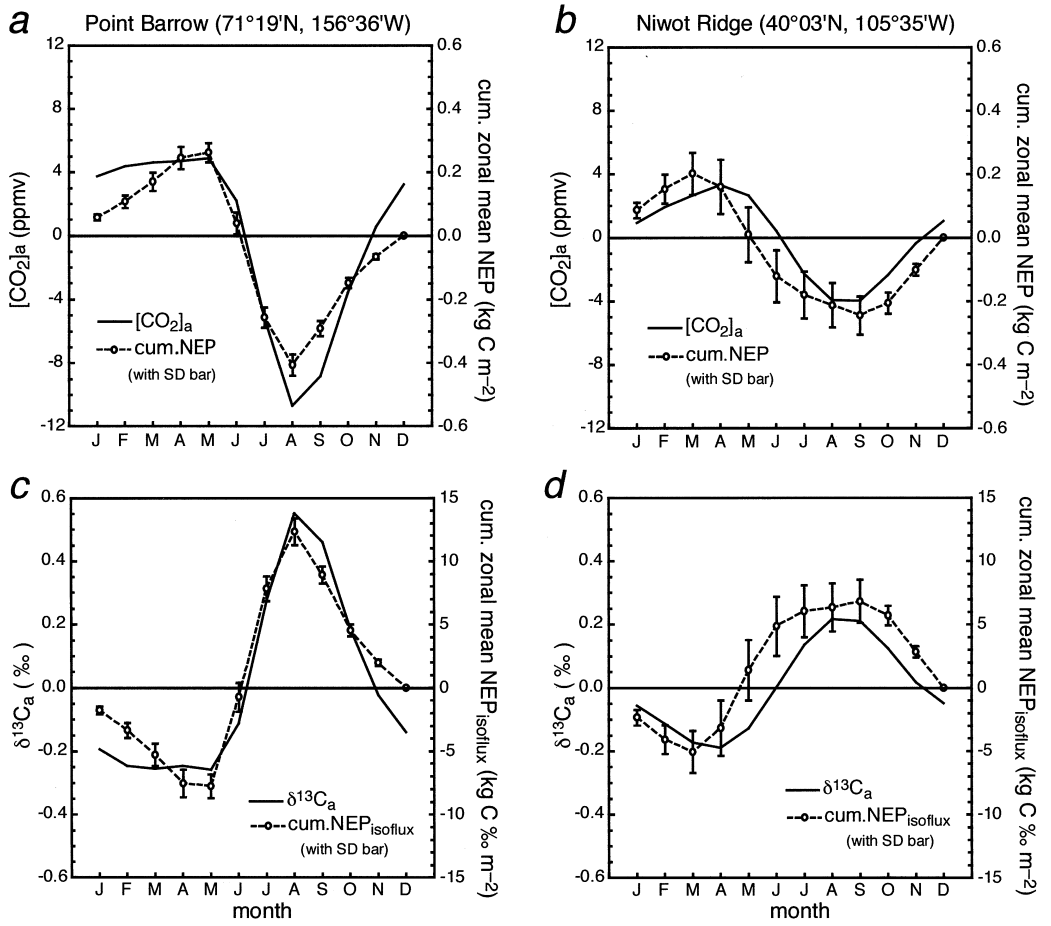

Fig. 8. Comparison between the observed atmospheric CO_2 trends and the estimated atmosphere–biosphere CO_2 exchange, left (a and c), at Point Barrow, Alaska and right (b and d), at Niwot Ridge, Colorado. Upper panels (a and b), cumulative monthly NEP and atmospheric CO_2 concentration; and lower panels (c and d), cumulative monthly $NEP_{isoflux}$ and atmospheric $\delta^{13}C_a - CO_2$. The average over 1990–1997, normalized by subtracting the annual-mean value, is shown (model estimates show standard-deviation bars for the interannual variability during the experimental period).

latitudes in the Northern Hemisphere. The estimated NEP and $NEP_{isoflux}$ approximately captured the seasonal trend, at both the northern high (Point Barrow) and middle latitudes (Niwot Ridge) (Fig. 8). At Point Barrow, a steep decrease of $[CO_2]_a$ and an increase in $\delta^{13}C_a$ from May to August were observed and simulated. On the other hand, at Niwot, Ridge, the model estimated an earlier onset of the phase shift, in March, than the observed onset in April. Moreover, the simulation estimates, at least qualitatively, a larger seasonal amplitude at the higher–latitude site (Point Barrow). Although generally we should take care that the observations are representative of the zonal CO_2 exchange, the comparison presented here offer some evidence supporting the model's validity.

3.5. *Interannual variability*

An analysis of the relationship between interannual climatic perturbations and anomalies in the CO_2 budget is regarded as an effective approach to exploring the responsiveness of terrestrial ecosystems to environmental change (Maisongrande et al., 1995; Ito and Oikawa, 2000a, b). Both photosynthetic and respiratory CO_2 flux varied substantially year by year, and a continuously increasing trend was induced by the

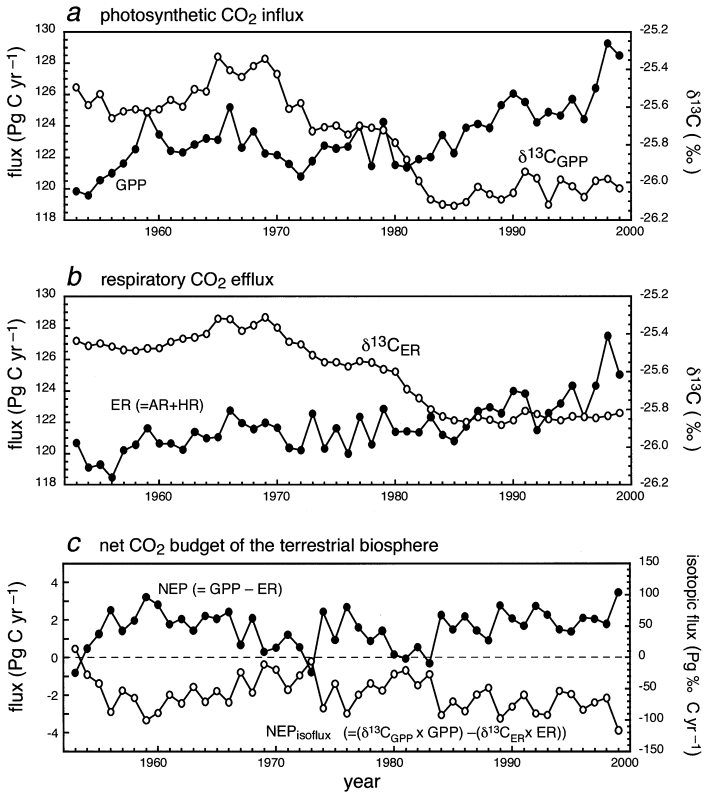

Fig. 9. Interannual change in atmosphere–biosphere CO_2 exchange rates and their stable carbon isotope ratios, with respect to (a) photosynthetic CO_2 uptake, (b) respiratory CO_2 release and (c) net CO_2 budget derived from a and b.

atmospheric CO_2 fertilization effect and climate change (Figs. 9a and 9b). The relationship between climatic perturbations (e.g. an El Niño event) and anomalies in carbon fluxes has already been fully analyzed by Ito and Oikawa (2000a, b). They showed that the estimated CO_2 fluxes responded to obvious climatic perturbations, such as the strong El Niño events in 1973, 1983 and 1998. As a result, NEP and $NEP_{isoflux}$ showed a substantial range of interannual variability (Fig. 9c). NEP was estimated as positive (i.e. a net carbon sink) for almost the entire experimental period, whereas the strong El Niño events in 1973 and 1983 resulted in negative NEP values. It is important to note that interannual changes in NEP and $NEP_{isoflux}$ howed a close correlation ($r^2 = 0.91$) but in opposite phase. Actually, a long-term observation of $[CO_2]_a$ and $\delta^{13}C_a$ in the western Pacific (Nakazawa et al., 1997) clarified that these parameters exhibited opposite interannual changes, suggesting that they reflect the contribution of the terrestrial biosphere. However, at present it is uncertain whether the estimated $NEP_{isoflux}$ can account for the flattening of the $\delta^{13}C$ decrease from 1988 to 1990 observed at Cape Grim by Francey et al. (1995).

The photosynthetic fractionation coefficient Δ was almost stable throughout the experimental period: interannual variability was generally within 1‰ (Fig. 10). We found no significant long-term trend in Δ, in spite of the rapid changes in atmospheric CO_2 parameters. In other words, the $[CO_2]_i/[CO_2]_a$ ratio was nearly stable throughout the experimental period, as has been suggested by ecophysiological studies (Ehleringer and Cerling, 1995). The interannual stability of Δ suggests that a double-deconvolution analysis using a constant Δ value may not result in a significant underestimation of the interannual variability of the terrestrial and oceanic CO_2 budgets. On the other hand, the apparent latitudinal change in Δ may call into question the spatial representativeness of $[CO_2]_a$ and $\delta^{13}C_a$ data used in double deconvolution studies (Keeling et al., 1995).

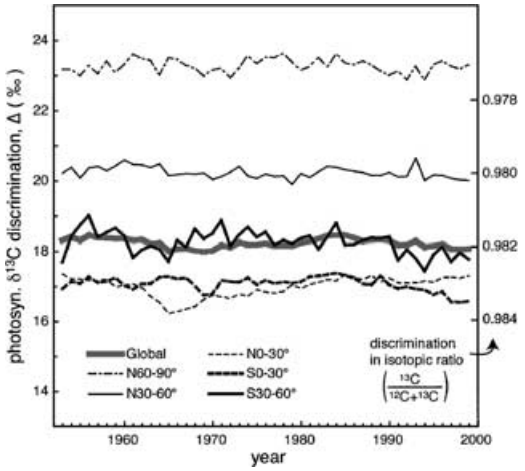

Fig. 10. Estimated interannual changes in the photosynthetic δ^{13}C-discrimination coefficient (Δ) of the terrestrial biosphere. Zonal and global average values are shown.

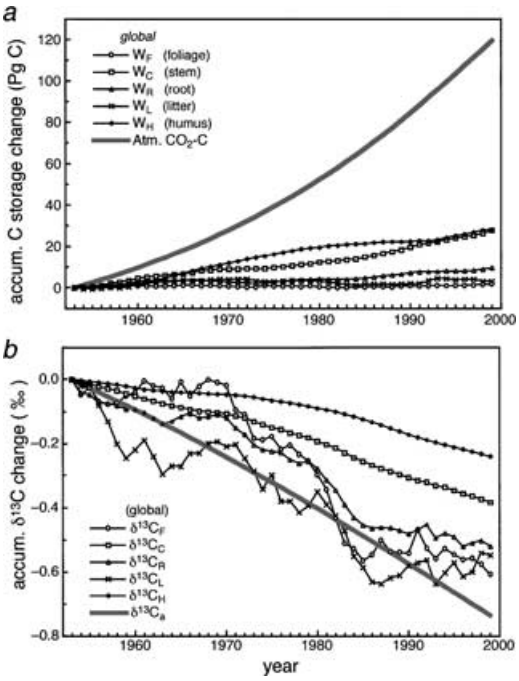

Fig. 11. Estimated changes in (a) atmospheric and biospheric carbon storage, and (b) the stable carbon isotope ratio (δ^{13}C) of carbon pools accumulated from 1953 to 1999. Note that the atmospheric CO_2 values are taken from a prescribed scenario, based on observational data (see text).

As shown in Fig. 11a, the terrestrial biosphere accumulated carbon through the experimental period, 38.5 Pg C in plant biomass and 31.5 Pg C in soil organic matter. This sequestration is equivalent to about 57% of the atmospheric CO_2 increase (120 Pg C), and 33% of the fossil fuel CO_2 emissions (210 Pg C; Andres et al., 1999) during the experimental period. The net sink mostly occurred in forest ecosystems, particularly in the Northern Hemisphere. On the other hand, δ^{13}C in carbon pools decreased, but at different rates (Fig. 11b). In a comparison between the first and the last 10 yr of the experiment (Table 2), it can been seen that biospheric δ^{13}C decreased by 0.3‰, which was less than half the decrease in $\delta^{13}C_a$. Although carbon pools with shorter MRTs (foliage, litter and roots) indicate a comparable rate of δ^{13}C decrease, plant stems and soil humus, which have longer MRTs, responded reluctantly. Additionally, the faster pools show interannual fluctuations, in response to climatic perturbations affecting C_3/C_4 composition and $[CO_2]_i/[CO_2]_a$ ratio. As a result of the different responsiveness between litter and humus, the difference between $\delta^{13}C_L$ and $\delta^{13}C_H$ was magnified from 0.2‰ in 1953 to 0.6‰ in 1999.

Tree-ring analyses may provide evidence for decreased biomass δ^{13}C during recent decades, although biomass δ^{13}C can vary in response to both atmospheric and plant physiological changes (Francey and Farquhar, 1982; Leavitt, 1994; Monserud and Marshall, 2001). For example, Stuiver et al. (1984) analyzed samples of spruce from Alaska, and demonstrated that woody δ^{13}C decreased from -23‰ in 1880 to -26.5‰ in 1980. Some evidence can also be obtained from archived plant materials; for example, Zhao et al. (2001) showed that the δ^{13}C of wheat grain and straw samples collected since 1845 decreased by about -2‰. From this evidence, we can reasonably deduce that δ^{13}C values of GPP and stored carbon decreased during the recent decades (Figs. 9 and 11), although there remains an uncertainty in the temporal agreement of the decrement rate. With respect to the δ^{13}C change in soil organic matter, Ehleringer et al. (2000) summarized the vertical distribution of δ^{13}C with depth in terms of atmospheric change and biological fractionation processes. They stated that the historical decrease in $\delta^{13}C_a$ may be the primary cause of the observed increase in δ^{13}C with soil depth, and that decomposition by microorganisms may amplify the vertical gradient.

3.6. Comparison with other studies and caveats

By comparing with other estimates, it was found that the general features of terrestrial carbon dynamics (storage and flux) were appropriately captured by Sim-CYCLE. For example, the average NPP of 62.1 Pg C yr^{-1} obtained by Sim-CYCLE is feasible, compared with other 16 model estimations (Cramer et al., 1999). However, the existing models give a wide range of NPP values (40–80 Pg C yr^{-1}), and then further constraints are needed for model validation. The estimated photosynthetic $\delta^{13}C$ discrimination, 18.2‰, is slightly larger than those obtained by other model studies: 14.8‰ by Lloyd and Farquhar (1994), 15.7‰ by Fung et al. (1997), 16.4‰ by François et al. (1999), and 15.6‰ by Buchmann and Kaplan (2001). However, the leaf-level discrimination (Δ_{leaf}) value of 16.1‰ is close to these previously obtained values. The previous sensitivity analysis suggests that uncertainty in stomatal conductance may not account for the difference between Δ values (about 2‰), and then inclusion of the canopy recycling may be chiefly responsible for the larger biospheric discrimination effect. As mentioned above, the estimated C_4-plant contribution to global GPP and spatial distribution of Δ were consistent with those of other model studies. In summary, the simulation with a process-based model gave a realistic estimation of the atmosphere–biosphere exchange of CO_2 and its stable carbon isotope ratio.

There remain, however, several methodological problems in the present research. (1) A stationary biome and land-use distribution was assumed, in spite of accelerating land-use change in the developing countries. (2) Ecosystem disturbances, such as wildfire and deforestation, were not included in the model, leading to overestimated MRTs for carbon pools. (3) Sim-CYCLE regards canopy as a mono-layer big-leaf, and it therefore does not explicitly express the vertical $\delta^{13}C$ gradient of leaves within a canopy (Hanba et al., 1997). Moreover, several observations show that there is an inter-species variability in $\delta^{13}C$ value within a plot (Hemming et al., 1998), suggesting a limitation of the compartment–model approach. (4) The simulation period (47 yr) may not be sufficiently long, compared with the turnover rate of biospheric carbon (up to millennia). Then, there remains uncertainty in the estimated $\delta^{13}C$ values of carbon pools with slow turnover rates. (5) The model needs further examination with respect to whether the leaf-level $\delta^{13}C$ discrimination, formulated by eqs. (5) and (6), is applicable to all C_3 and C_4 species, irrespective of biome type. (6) Additional validation is also needed for the agreement between estimated NEP and observed atmospheric CO_2 seasonality, although it still has intrinsic and practical limitations (Knorr and Heimann, 2001b). In spite of these caveats, this study carries several implications, as follows.

3.7. Implications

It is clear that in many terrestrial ecosystems, carbon storage data indicate a mean residence time of several decades or centuries (Fig. 2c). This implies that some fraction of respired carbon could have sequestered from the past atmosphere during the preindustrial era. As a result, an isotopic disequilibrium may occur between the two carbon pools, the atmosphere and the biosphere (i.e., the ^{13}C Suess effect). Based on the definition of Tans et al. (1993), the flux-weighted isotopic disequilibrium can be calculated as 23.7 ± 5.9 Pg C ‰ yr^{-1} from the present model simulation. This value seems close to other estimations: 25.8 Pg C ‰ yr^{-1} by Francey et al. (1995), 23.4 Pg C ‰ yr^{-1} by Heimann and Maier-Reimer (1996), and 27.2 Pg C ‰ yr^{-1} by Morimoto et al. (2000), but slightly larger than the 18.0 Pg C ‰ yr^{-1} estimated by Wittenberg and Esser (1997). The critical implication of the model simulation is the wide range of interannual variability (SD $\pm$5.9 Pg C ‰ yr^{-1}). Heimann and Maier-Reimer (1996) performed a sensitivity analysis for the parameters used in double-deconvolution studies, and concluded that the ^{13}C Suess effect was one of the most influential parameters on accuracy. Although the present simulation suggests that a constant Δ value through time may be reasonable for double–deconvolution studies, variability in the disequilibrium term should be considered in analyses of interannual change. The spatial and temporal distribution of the disequilibrium term (cf. Fung et al., 1997; Ciais et al., 1999), not presented here, will be described in detail in a forthcoming analysis.

Terrestrial carbon cycle models have already been coupled with atmospheric transport models in several studies (Heimann et al., 1998), allowing us to validate terrestrial models by using atmospheric data. Similarly, the inclusion of the $\delta^{13}C$ ratio into the coupled atmosphere–terrestrial model will allow us to validate additional features related to isotopic characteristics of terrestrial CO_2 exchange, such as the C_3/C_4 distribution ratio and the mean residence time of carbon. This may lead to improved precision in quantifying

the global carbon cycle, in relation to global environmental change. Actually, field experiments and observations suggest that elevated $[CO_2]_a$ can alter stomatal gas exchange, leaf area index, and C_3/C_4 ratio (Bazzaz, 1996; Collatz et al., 1998), all of which are more or less related to terrestrial NEP and $\delta^{13}C$ discrimination. From this study, it was found that the spatial heterogeneity in Δ was mainly attributable to the distribution of C_3 and C_4 plants (Figs. 2 and 5); this may imply that C_3/C_4 composition may largely influence the long-term variation in the biospheric $\delta^{13}C$ discrimination effect. Therefore, establishing a model of C_3/C_4 composition, as well as a stomatal conductance model, is essential for elucidating the terrestrial carbon dynamics.

4. Conclusion

This study presents spatial and temporal patterns of the atmosphere–biosphere CO_2 exchange, incorporating the stable carbon isotopic ratio, simulated with a process-based model. This is one of a few attempts to address spatial, seasonal and interannual patterns of terrestrial carbon dynamics, on a basis of reliable climatic data. The model was designed to estimate CO_2 and $\delta^{13}C$ exchange with comparable precision, because the double-deconvolution method demands precise information on both $[CO_2]_a$ and $\delta^{13}C_a$. The present simulation, at least of the past 47 yr, implies that the terrestrial biosphere is sensitive to global environmental changes, such as increasing atmospheric CO_2 and climatic perturbations. The present simulation also emphasized the spatial heterogeneity of terrestrial ecosystems, in the carbon exchange rate, carbon storage and the isotopic discrimination effect.

Further interdisciplinary studies will be required to refine our understanding of the carbon cycle, particularly with respect to stable carbon isotopes: to determine the leaf-level discrimination, we need ecophysiological studies; to determine the canopy-level CO_2 recycling, we need micrometeorological methods; and to determine C_3/C_4 distribution, we need ecological surveys. For example, a flux observation by the eddy covariance method, coupled with the simultaneous measurement of $\delta^{13}C_a$, will be an effective approach, if it can be carried out in a wide range of terrestrial environments. In conclusion, additional modeling research is needed to further elucidate the atmosphere–biosphere exchange and its stable carbon isotope ratio of CO_2.

5. Acknowledgements

The present author is grateful to Dr. S. Morimoto and Dr. T. Nakazawa for their suggestions with regard to this study, and to Dr. M. Stevens and Dr. S. Duhon for their assistance in preparing the manuscript. This work is a contribution to "The Frontier Research System for Global Change," which is supported by the Ministry of Education, Culture, Science, Sports and Technology of Japan.

REFERENCES

Ågren, G. I., Bosatta, E. and Balesdent, J. 1996. Isotope discrimination during decomposition of organic matter: a theoretical analysis. *Soil Sci. Soc. Am. J.* **30**, 1121–1126.

Andres, R. J., Fielding, D. J., Marland, G., Boden, T. A., Kumar, N. and Kearney, A. T. 1999. Carbon dioxide emissions from fossil-fuel use, 1751–1950. *Tellus* **51B**, 759–765.

Bakwin, P. S., Tans, P. P., White, J. W. C. and Andres, R. J. 1998. Determination of the isotopic ($^{13}C/^{12}C$) discrimination by terrestrial biology from a global network of observations. *Global Biogeochem. Cycles* **12**, 555–562.

Battle, M., Bender, M. L., Tans, P. P., White, J. W. C., Ellis, J. T., Conway, T. and Francey, R. J. 2000. Global carbon sinks and their variability inferred from atmospheric O_2 and $\delta^{13}C$. *Science* **287**, 2467–2470.

Bazzaz, F. A. 1996. *Plants in changing environment*. Cambridge University Press, Cambridge.

Bird, M. I., Chivas, A. R. and Head, J. 1996. A latitudinal gradient in carbon turnover times in forest soils. *Nature* **381**, 143–146.

Buchmann, N. and Kaplan, J. O. 2001. Carbon isotope discrimination of terrestrial ecosystems–How well do observed and modeled results match? In: *Global biogeochemical cycles in the climate system* (eds. E.-D. Schulze, M. Heimann, S. Harrison, E. Holland, J. Lloyd, I. C. Prentice and D. Schimel). Academic Press, San Diego, 253–266.

Caldwell, M. M., White, R. S., Moore, R. T. and Camp, L. B. 1977. Carbon balance, productivity, and water use of cold-winter desert shrub communities dominated by C_3 and C_4 species. *Oecologia* **29**, 275–300.

Cavagnaro, J. B. 1988. Distribution of C_3 and C_4 grasses at different altitudes in a temperate arid region of Argentina. *Oecologia* **76**, 273–277.

Ciais, P., Tans, P. P., White, J. W. C., Trolier, M., Francey, R. J., Berry, J. A., Randall, D. R., Sellers, P. J., Collatz, J. G. and Schimel, D. S. 1995. Partitioning of ocean and land uptake of CO_2 as inferred by $\delta^{13}C$ measurements from the NOAA Climate Monitoring and Diagnostics Laboratory Global Air Sampling Network. *J. Geophys. Res.* **100**, 5051–5070.

Ciais, P., Friedlingstein, P., Schimel, D. S. and Tans, P. P. 1999. A global calculation of the $\delta^{13}C$ of soil respired carbon: implications for the biospheric uptake of anthropogenic CO_2. *Global Biogeochem. Cycles* **13**, 519–530.

Collatz, G. J., Berry, J. A. and Clark, J. S. 1998. Effects of climate and atmospheric CO_2 partial pressure on the global distribution of C_4 grasses: present, past, and future. *Oecologia* **114**, 441–454.

Cramer, W., Kicklighter, D. W., Bondeau, A., Moore, B. III., Churkina, G., Nemry, B., Ruimy, A., Schloss, A. L. and Potsdam NPP model intercomparison participants 1999. Comparing global NPP models of terrestrial net primary productivity (NPP): overview and key results. *Global Change Biol.* **5** (suppl. 1), 1–15.

Ehleringer, J. R. and Cerling, T. E. 1995. Atmospheric CO_2 and the ratio of intercellular to ambient CO_2 concentration in plants. *Tree Physiol.* **15**, 105–111.

Ehleringer, J. R., Cerling, T. E. and Helliker, B. R. 1997. C_4 photosynthesis, atmospheric CO_2, and climate. *Oecologia* **112**, 285–299.

Ehleringer, J. R., Buchmann, N. and Flanagan, L. B. 2000. Carbon isotope ratios in belowground carbon cycle processes. *Ecol. Appl.* **10**, 412–422.

Epstein, H. E., Lauenroth, W. K., Burke, I. C. and Coffin, D. P. 1997. Productivity patterns of C_3 and C_4 functional types in the U.S. Great Plains. *Ecology* **78**, 722–731.

Etheridge, D. M., Steele, L. P., Langenfelds, R. L., Francey, R. J., Barnola, J.-M. and Morgan, V. I. 1996. Natural and anthropogenic changes in atmospheric CO_2 over the last 1000 years from air in Antarctic ice and firn. *J. Geophys. Res.* **101**, 4115–4128.

Farquhar, G. D., Ehleringer, J. R. and Hubick, K. T. 1989. Carbon isotope discrimination and photosynthesis. *Annu. Rev. Plant Physiol. Plant Mol. Biol.* **40**, 503–537.

Francey, R. J. and Farquhar, G. D. 1982. An explanation of $^{13}C/^{12}C$ variations in tree rings. *Nature* **297**, 28–31.

Francey, R. J., Tans, P. P., Allison, C. E., Enting, I. G., White, J. W. C. and Trolier, M. 1995. Changes in oceanic and terrestrial carbon uptake since 1982. *Nature* **373**, 326–330.

Francey, R. J., Allison, C. E., Etheridge, D. M., Trudinger, C. M., Enting, I. G., Leuenberger, M., Langenfelds, R. L., Michel, E. and Steele, L. P. 1999. A 1000-year high precision record of $\delta^{13}C$ in atmospheric CO_2. *Tellus* **51B**, 170–193.

François, L. M., Godderis, Y., Warnant, P., Ramstein, G., de Noblet, N. and Lorenz, S. 1999. Carbon stocks and isotopic budgets of the terrestrial biosphere at mid-Holocene and last glacial maximum times. *Chem. Geol.* **159**, 163–189.

Friedli, H., Lotscher, H., Oeschger, H., Siegenthaler, U. and Stauffer, B. 1986. Ice core record of the $^{13}C/^{12}C$ ratio of atmospheric CO_2 in the past two centuries. *Nature* **324**, 237–238.

Fung, I., Field, C. B., Berry, J. A., Thompson, M. V., Randerson, J. T., Malmstrom, C. M., Vitousek, P. M., Collatz, G. J., Sellers, P. J., Randall, D. A., Denning, A. S., Badeck, F. and John, J. 1997. Carbon-13 exchanges between the atmosphere and biosphere. *Global Biogeochem. Cycles* **11**, 507–533.

GLOBALVIEW-CO_2 2000. Atmospheric CO_2 concentration dataset. NOAA/CMDL.

Hanba, Y. T., Mori, S., Lei, T. T., Koike, T. and Wada, E. 1997. Variations in leaf $\delta^{13}C$ along a vertical profile of irradiance in a temperate Japanese forest. *Oecologia* **110**, 253–261.

Hattersley, P. W. 1983. The distribution of C_3 and C_4 grasses in Australia in relation to climate. *Oecologia* **57**, 113–128.

Heimann, M. and Maier-Reimer, E. 1996. On the relations between the oceanic uptake of CO_2 and its carbon isotopes. *Global Biogeochem. Cycles* **10**, 89–110.

Heimann, M., Esser, G., Haxeltine, A., Kaduk, J., Kicklighter, D. W., Knorr, W., Kohlmaier, G. H., McGuire, A. D., Melillo, J., Moore, B. I., Otto, R. D., Prentice, I. C., Sauf, W., Schloss, A., Sitch, S., Wittenberg, U. and Wurth, G. 1998. Evaluation of terrestrial carbon cycle model through simulations of the seasonal cycle of atmospheric CO_2: First results of a model intercomparison study. *Global Biogeochem. Cycles* **12**, 1–24.

Hemming, D. L., Switsur, V. R., Waterhouse, J. S., Heaton, T. H. E. and Carter, A. H. C. 1998. Climate variation and the stable carbon isotope composition of tree ring cellulose: and intercomparison of *Quercus robur, Fagus sylvatica* and *Pinus silvestris. Tellus* **50**, 25–33.

Ito, A. and Oikawa, T. 2000a. The large carbon emission from terrestrial ecosystems in 1998: a model simulation. *J. Meteorol. Soc. Jpn*. **78**, 103–110.

Ito, A. and Oikawa, T. 2000b. A model analysis of the relationship between climate perturbations and carbon budget anomalies in global terrestrial ecosystems: 1970–1997. *Clim. Res.* **15**, 161–183.

Ito, A. and Oikawa, T. 2002. A simulation model of the carbon cycle in land ecosystems (Sim-CYCLE): A description based on dry-matter production theory and plot-scale validation. *Ecol. Model*. **151**, 143–176.

Keeling, C. D. 1961. A mechanism for cyclic enrichment of carbon-12 by terrestrial plants. *Geochim. Cosmochim. Acta* **24**, 299–313.

Keeling, C. D. and Whorf, T. P. 2000. Atmospheric CO_2 concentrations–Mauna Loa Observatory, Hawaii, 1958–1999. Oak Ridge National Laboratory, Oak Ridge, TN, USA.

Keeling, C. D., Bacastow, R. B., Carter, A. F., Piper, S. C., Whorf, T. P., Heimann, M., Mook, W. G. and Roeloffzen, H. 1989. A three-dimensional model of atmospheric CO_2 transport based on observed winds: 1. Analysis of observational data. *Geophys. Monogr*. **55**, 165–236.

Keeling, C. D., Whorf, T. P., Wahlen, M. and van der Plicht, J. 1995. Interannual extremes in the rate of atmospheric carbon dioxide since 1980. *Nature* **375**, 666–670.

Knorr, W. and Heimann, M. 2001a. Uncertainties in global terrestrial biosphere modeling 1. A comprehensive sensitivity analysis with a new photosynthesis and energy balance scheme. *Global Biogeochem. Cycles* **15**, 207–225.

Knorr, W. and Heimann, M. 2001b. Uncertainties in global terrestrial biosphere modeling Part II. Global constraints for a process-based vegetation model. *Global Biogeochem. Cycles* **15**, 227–246.

Körner, C., Farquhar, G. D. and Wong, S. C. 1991. Carbon isotope discrimination by plants follows latitudinal and altitudinal trends. *Oecologia* **88**, 30–40.

Leavitt, S. W. 1994. South American tree rings show declining $\delta^{13}C$ trend. *Tellus* **46B**, 152–157.

Leuning, R. 1990. Modelling stomatal behavior and photosynthesis of *Eucalyptus grandis*. *Aust. J. Plant Physiol*. **17**, 159–175.

Lin, G. and Ehleringer, J. R. 1997. Carbon isotopic fractionation does not occur during dark respiration in C_3 and C_4 plants. *Plant Physiol.* **114**, 391–394.

Lloyd, J. and Farquhar, G. D. 1994. ^{13}C discrimination during CO_2 assimilation by the terrestrial biosphere. *Oecologia* **99**, 201–215.

Lloyd, J., Kruijt, B., Hollinger, D. Y., Grace, J., Francey, R. J., Wong, S.-C., Kelliher, F. M., Miranda, A. C., Farquhar, G. D., Gash, J. H. C., Vygodskaya, N. N., Wright, I. R., Miranda, H. S. and Schulze, E.-D. 1996. Vegetation effects on the isotopic composition of atmospheric CO_2 at local and regional scales: theoretical aspects and a comparison between rain forest in Amazonia and a boreal forest in Siberia. *Aust. J. Plant Physiol*. **23**, 371–399.

Maisongrande, P., Ruimy, A., Dedieu, G. and Saugier, B. 1995. Monitoring seasonal and interannual variations of gross primary productivity, net primary productivity and net ecosystem productivity using a diagnostic model and remotely-sensed data. *Tellus* **47B**, 178–190.

Matthews, E. 1983. Global vegetation and land use: new high resolution data bases for climate studies. *J. Clim. App. Meteorol*. **22**, 474–487.

Monserud, R. A. and Marshall, J. D. 2001. Time-series analysis of $\delta^{13}C$ from tree rings. I. Time trends and autocorrelation. *Tree Physiol.* **21**, 1087–1102.

Morimoto, S., Nakazawa, T., Higuchi, K. and Aoki, S. 2000. Latitudinal distribution of atmospheric CO_2 sources and sinks inferred by $\delta^{13}C$ measurements from 1985 to 1991. *J. Geophys. Res.* **105**, 24315–24326.

Nakazawa, T., Morimoto, S., Aoki, S. and Tanaka, M. 1997. Temporal and spatial variations of the carbon isotopic ratio of atmospheric carbon dioxide in the western Pacific region. *J. Geophys. Res.* **102**, 1271–1285.

O'Leary, M. H., Treichel, I. and Rooney, M. 1986. Short-term measurement of carbon isotope fractionation in plants. *Plant Physiol.* **80**, 578–582.

Paruelo, J. M. and Lauenroth, W. K. 1996. Relative abundance of plant functional types in grassland and shrublands of North America. *Ecol. Appl.* **6**, 1212–1224.

Prentice, I. C. 2001. The carbon cycle and atmospheric carbon dioxide. In: *Climate Change 2001: The scientific basis* (eds. J. T. Houghton, Y. Ding, D. J. Griggs, M. Noguer, P. J. van der Linden, X. Dai, K. Maskell and C. W. Johnson). Cambridge University Press, Cambridge, 183–237.

Rayner, P. J., Enting, I. G., Francey, R. J. and Langenfelds, R. 1999. Reconstructing the recent carbon cycle from atmospheric CO_2, $\delta^{13}C$ and O_2/N_2 observations. *Tellus* **51B**, 213–232.

Sage, R. F., Wedin, D. A. and Li, M. 1999. The biogeography of C_4 photosynthesis: patterns and controlling factors. In: *C_4 plant biology* (eds. R. F. Sage and R. K. Monson). Academic Press, San Diego, 313–373.

Saigusa, N., Liu, S., Oikawa, T. and Watanabe, T. 1996. Seasonal change in CO_2 and H_2O exchange between grassland and atmosphere. *Ann.Geophys.* **14**, 342–350.

Sitch, S. 2000. *The role of vegetation dynamics in the control of atmospheric CO_2 content.* Ph.D. dissertation, Lund University, Lund, Sweden.

Sternberg, L. d. S. L., Moreira, M. Z., Martinelli, L. A., Victoria, R. L., Barbosa, E. M., Bonates, L. C. M. and Nepstad, D. C. 1997. Carbon dioxide recycling in two Amazonian tropical forests. *Agr. For. Meteorol*. **88**, 259–268.

Stuiver, M., Burk, R. L. and Quay, P. D. 1984. $^{13}C/^{12}C$ ratios in tree rings and the transfer of biospheric carbon to the atmosphere. *J. Geophys. Res.* **89**, 11731–11748.

Takeda, T., Takikawa, T., Agata, W. and Hakoyama, S. 1985. Studies on the ecology and geographical distribution of C_3 and C_4 grasses. II. Geographical distribution of C_3 and C_4 grasses in Far East and South East Asia. *Jpn. J. Crop Sci*. **54**, 65–71.

Tans, P. P., Berry, J. A. and Keeling, R. F. 1993. Oceanic $^{13}C/^{12}C$ observations: a new window on oceanic CO_2 uptake. *Global Biogeochem. Cycles* **7**, 353–368.

Teeri, J. A. and Stowe, L. G. 1976. Climatic patterns and the distribution of C_4 grasses in North America. *Oecologia* **23**, 1–12.

Tieszen, L. L., Senyimba, M. M., Imbamba, S. K. and Throughton, J. H. 1979. The distribution of C_3 and C_4 grasses and carbon isotope discrimination along an altitudinal and moisture gradient in Kenya. *Oecologia* **37**, 337–350.

Tieszen, L. L., Reed, B. C., Bliss, N. B., Wylie, B. K. and DeJong, D. D. 1997. NDVI, C_3 and C_4 production, and distributions in Great Plains grassland land cover classes. *Ecol. Appl.* **7**, 59–78.

Winter, K. 1981. C_4 plants of high biomass in arid regions of Asia—occurrence of C_4 photosynthesis in Chenopodiacea and Polygonaceae from the Middle East and USSR. *Oecologia* **48**, 100–106.

Wittenberg, U. and Esser, G. 1997. Evaluation of the isotopic disequilibrium in the terrestrial biosphere by a global carbon isotope model. *Tellus* **49B**, 263–269.

Zhao, E.-J., Spiro, B. and McGrath, S. P. 2001. Trends in $^{13}C/^{12}C$ ratios and C isotope discrimination of wheat since 1845. *Oecologia* **128**, 336–342.